International Journal Of

Recent Scientific Research

ISSN: 0976-3031

Volume: 7(2) February -2016

U-SERIES RADIONUCLIDES DISEQUILIBRIA AS INDICATION OF RECENT U-MOBILIZATION IN THE METAMORPHOSED SANDSTONE, WADI SIKAIT, SOUTH EASTERN DESERT, EGYPT

Eman M. Ibrahim., Sayed F. Hassan and Mohamed G. El Feky

THE OFFICIAL PUBLICATION OF
INTERNATIONAL JOURNAL OF RECENT SCIENTIFIC RESEARCH (IJRSR)
http://www.recentscientific.com/ recentscientific@gmail.com

ISSN: 0976-3031

Available Online at http://www.recentscientific.com

International Journal of Recent Scientific Research
Vol. 7, Issue, 2, pp. 8849-8858, February, 2016

International Journal of Recent Scientific Research

RESEARCH ARTICLE

U-SERIES RADIONUCLIDES DISEQUILIBRIA AS INDICATION OF RECENT U-MOBILIZATION IN THE METAMORPHOSED SANDSTONE, WADI SIKAIT, SOUTH EASTERN DESERT, EGYPT

Eman M. Ibrahim., Sayed F. Hassan and Mohamed G. El Feky

Nuclear Materials Authority, P.O. Box: 530, El-Maadi, Cairo, Egypt

ARTICLE INFO

Article History:

Received 06th November, 2015
Received in revised form 14th December, 2015
Accepted 23rd January, 2016
Published online 28th February, 2016

Key words:

Radionuclides, Metamorphosed Sandstone, Age Dating, Wadi Sikait

ABSTRACT

Specific activity and activity ratios of different radionuclides in uranium series were measured by HPGe-detector for 14 metamorphosed sandstone samples. The $^{232}Th/^{238}U$ concentration ratios are ranging between 0.12 and 3.14 which indicate U migration-in. The ratios between nuclides of U-series showed obvious deviations from secular equilibrium, indicating the deposition of uranium during the last 1 Ma and of radium during the last 8×10^3 yr. The shear zones represent channels for ground- and surface water flow, where the migration of uranium-series radionuclides along the fracture zones may be due to adsorption onto the alteration products (clays, iron oxides) of the surrounding rocks or by later mobility by ground and surface water. The calculated ages of metamorphosed sandstone samples indicate major U accumulation in age ranges between 109.6 and 460.1 ky ago for Sikait-1 and between 57.97 and 211.8 ky ago for Sikait-2. The $^{230}Th/^{232}Th$ activity ratios range between 0.65 and 22.15 for Sikait-1 samples and between 0.79 and 2.49 for Sikait-2 samples which are smaller than 20 except one sample (S8), indicating a contamination of the samples by detrital ^{230}Th. So, after subtraction the detrital ^{230}Th, the corrected age for Sikait-1 samples vary from 97.17 to 441.9 kyr while for Sikait-2 samples vary from 53.71 to 201.1 kyr. These ages are conformable with U-series ages reported for secondary uranium minerals in the eastern and western deserts and indicate that there is more than one phase of uranium mineralization in the studied area.

INTRODUCTION

^{238}U is the most abundant U isotope (99.2745 %), and ^{232}Th is the most abundant Th isotope (~100 %). The average Th/U weight ratio in crustal rocks is ~3.5 (Wedepohl, 1995). The half-lives of ^{238}U ($T_{1/2} = 4.4683 \times 10^9$ a), ^{235}U ($T_{1/2} = 0.70381 \times 10^9$ a), and ^{232}Th ($T_{1/2} = 14.01 \times 10^9$ a) are much longer than those of their daughters in the decay chain. Thus, the activities of parent and daughter isotopes reach a state of secular equilibrium in naturally occurring undisturbed materials within several million years. However, natural processes can disrupt the state of equilibrium, which is the key of the U-series disequilibrium dating methods. A state of disequilibrium in the ^{238}U decay chain can either result from the different geochemical behaviour of U and Th or from isotope fractionation between ^{234}U and ^{238}U produced by the α-recoil effect (Scholz and Hoffmann, 2008).

Uranium mainly exists in two oxidation states in nature (U^{4+} and U^{6+}), and at the Earth's surface it is dominant in its soluble U^{6+} form. It is soluble as uranyl ion $(UO_2)^{2+}$ and in various uranyl carbonate forms. In a reducing environment, it occurs mainly in the U^{4+} state where it is insoluble and, thus, far less mobile than U^{6+}. In contrast, Th, which occurs in terrestrial material mainly in the 4+ oxidation state, is insoluble in natural waters (Ivanovich and Harmon, 1992), and, under natural conditions usually transported in minerals or adsorbed onto particles. Hence, in contrast to U, Th is not incorporated in secondary carbonates during their formation resulting in an initial Th/U disequilibrium (Scholz and Hoffmann, 2008).

In environmental systems, fractionation of uranium and thorium is a very efficient process because thorium is extremely insoluble while hexavalent uranium in oxidising conditions is relatively soluble (Calsteren and Thomas, 2006).

The uranium-series dating method is based on the measurement of the activity of uranium and its various daughter nuclides. In any naturally occurring material which contains uranium and which has remained undisturbed for several million years, a state of secular equilibrium between the parent and the daughter nuclide in the radioactive series would have been

Corresponding author:* **Eman M. Ibrahim
Nuclear Materials Authority, P.O. Box: 530, El-Maadi, Cairo, Egypt

established. However, when a deposit is formed, various geochemical processes occur causing isotopic and elemental fractionation and initiating a state of disequilibrium. The uranium-series dating method incorporates multiple parent–daughter decay pairs. One of these schemes is based on accumulation of decay products of uranium (daughter deficiency method). In this method, a parent nuclide may be deposited free of its daughters or a daughter deficiency of known extent may be established, so that at some subsequent time, the age of the deposit can be determined from the extent of growth of the daughter into secular equilibrium with its parent. In the present study, the $^{230}Th/^{234}U$ dating method is used where the formation of secondary uranium deposits was associated with daughter deficiency. In practice, the dating range of this method is considered to be around 350 ka to the present (Dawood *et al*., 2014).

Pluvial periods of Late Quaternary were indicated in the Eastern Desert of Egypt by dating uranyl mineralization (Osmond and Dabous 2004). Apparently, pluvial conditions caused the mobilization and redeposition of the uranium by groundwater (Dawood *et al*., 2014). The U-series dating methods have been used for the Quaternary period.

U-series dating

The U-series dating method is based on the decay of ^{238}U ($t_{1/2}$=4.469 × 10^9 years) to stable ^{206}Pb via intermediate daughters such as ^{234}U ($t_{1/2}$=245000 years) and ^{230}Th ($t_{1/2}$=75400 years). In this decay series, ^{238}U–^{234}U–^{230}Th disequilibrium occurs when U is differentiated from Th during a particular geological or environmental event or process. Once disequilibrium is established, it takes about seven times the half life of ^{230}Th (~500 ka) for the system to return to near secular equilibrium (Zhao *et al*., 2009). Ages for authigenic minerals can be calculated for single samples on the assumption that all ^{230}Th has been produced by in situ decay of ^{234}U and there is no allogenic or initial ^{230}Th and no isotope redistribution within the system or exchange with the environment. The ages are determined from the following equation which was derived by Kaufman and Broecker (1965).

$$\left(\frac{^{230}Th}{^{234}U}\right) = \left(\frac{^{238}U}{^{234}U}\right) \times \left(1 - e^{-T\lambda_{230}}\right) + \left\{\lambda_{230}/(\lambda_{230}-\lambda_{234})\right\} \times \left\{1 - \left(\frac{^{238}U}{^{234}U}\right)\right\} \times \left\{1 - e^{-T(\lambda_{230}-\lambda_{234})}\right\} \quad \ldots\ldots\ldots(1)$$

where T is the age of the sample, ($^{230}Th/^{234}U$) and ($^{238}U/^{234}U$) are the measured activity ratios, and λ_{230} and λ_{234} are the decay constants of ^{230}Th and ^{234}U, respectively.

Uranium-thorium dating relies on the propensity of uranium, a very soluble element in oxidised groundwaters, to co-precipitate with calcium during carbonate formation, in the absence of its daughter, ^{230}Th, which is almost totally immobile in the near-surface environment (Langmuir and Herman, 1980). The subsequent in-growth ^{230}Th provides a chronometer with which to measure elapsed time since carbonate deposition. Age is calculated from the measured $^{230}Th/^{234}U$ and $^{234}U/^{238}U$ ratios in the sample (Ivanovich and Harmon, 1992; Rowe and Maher, 2000).

The in-growth of ^{230}Th to secular equilibrium with its parent ^{234}U takes ca. 350 ka and sets the upper age limit for the technique. Preconditions for the reliability of the calculated age are that no thorium should initially be present and that the carbonate must remain a closed system after deposition, allowing no isotopic migration across its boundaries. The presence of any initial thorium can be deduced from the presence of the cosmogenic isotope ^{232}Th and thus this potential source of error can be detected (Rowe and Maher, 2000).

A considerable source of uncertainty for U/Th dating is the correction for thorium that is not in-grown by radioactive decay, but is incorporated during carbonate formation. Isochrone techniques are powerful tools to minimize these uncertainties because they assume samples to be composed of two distinct phases. In the case of U/Th dating, one phase is supposed to contain all the initial thorium (detrital fraction) while the other carries only thorium produced by radioactive decay (authigenic fraction) (Wirsig *et al*., 2012).

If detrital materials are present in the carbonate, contamination by externally supplied ^{230}Th can occur which result in a deduced age greater than the true age. Because the detrital ^{230}Th is usually accompanied by ^{232}Th, the ^{232}Th is used as an index of the amount of externally supplied ^{230}Th. Generally, $^{230}Th/^{232}Th$ activity ratios greater than 20 indicate, in practice, the absence of detrital components (Choukri *et al*., 2007; Dawood *et al*., 2013). The effects of detrital contamination can be corrected by measuring the activity of ^{232}Th that is solely present in the detrital fraction but which plays no part in the decay chain of uranium (Taçon *et al*., 2012).

During aging ^{234}U has decayed to $^{230}Th^*$ (radiogenic). The activity of $^{230}Th^*$ is calculated from the measured total $^{230}Th_{total}$ activity (= Th^*(radiogenic) + Th (detrital)) using Eq. (2). The difference between the uncorrected $^{230}Th/U$ age calculated from the total $^{230}Th_{total}$ activity, and the detritus-corrected $^{230}Th^*/U$ age calculated from [$^{230}Th^*$] increases with Th index or the ^{232}Th activity growth, decreasing the age.

$$\left[^{230}Th_{total}\right] = \left[^{230}Th^*\right] + \left[\frac{^{230}Th}{^{232}Th}\right]\left[^{232}Th\right] = \left[^{230}Th^*\right] + f.\left[^{232}Th\right] \quad \ldots\ldots\ldots(2)$$

The slope of the straight mixing line (isochron) in the plot of $^{230}Th/^{232}Th$ AR versus $^{234}U/^{232}Th$ AR equals the actual $^{230}Th^*/^{234}U$ AR which is the crucial parameter to calculate $^{230}Th^*/U$ ages. The intersection of the isochron on the Y axis yields the present [$^{230}Th/^{232}Th$] AR or the present thorium index f (Geyh, 2001).

The most common methods to measure the amount of uranium and its daughter thorium in a sample are by mass-spectrometry and α-particle spectrometry. The present paper deals with the method of determining the important uranium isotopes and

daughters for dating by γ-ray spectrometry (Simpson and Grün, 1998). A non-destructive, gamma-spectrometric method for uranium age-dating is presented which is applicable to material of any physical form and geometrical shape. It relies on measuring the daughter/parent activity ratio $^{230}Th/^{234}U$ by high-resolution gamma-spectrometry using intrinsic efficiency calibration. The method does not require the use of any reference materials of known ages. It relies on evaluating the daughter/parent activity ratio $^{230}Th/^{234}U$, obtained by directly measuring the count rates of the relevant γ peaks of ^{230}Th and ^{234}U.

Several nuclides of the ^{238}U (^{234}Th, ^{234m}Pa, ^{234}U, ^{230}Th, ^{226}Ra and ^{210}Pb) decay series have been measured through gamma spectrometry in the U-bearing episyenites of the metamorphosed sandstones occur in two location at Wadi Sikait (Sikait-1 and Sikait-2), south Eastern Desert, Egypt, in order to study recent mobilizations in the U-deposit and their time-scales.

Sikait-Nugrus area is bordering to the major shear zone known as the Nugrus thrust fault (Greiling *et al*., 1988) or the Nugrus strike-slip fault (Fritz *et al*., 1996) and or Sha'it–Nugrus shear zone (Fowler and Osman, 2009). Wadi Sikait area is located at the Southern part of the Eastern Desert of Egypt, about 45km to the Southwest of Marsa Alam city. It is bounded by latitudes 24° 39′ 23" and 24° 40′ 12" N and longitudes 34° 46′ 34" and 34° 46′ 46" E.

Geological Setting

The studied area revealed that the metamorphosed sandstone occur in two location at Wadi Sikait [Sikait-1 and Sikait-2] (Fig. 1). The exposed rocks at Wadi Sikait can be arranged based on the field observations and structural relations from oldest to youngest as follows; Ophioltic mélange, Metamorphosed sandstone, Biotite granites, Lamprophyre dykes and Fluorite and quartz veins.

Metamorphosed sandstones

The metamorphosed sandstones occur in two locations in Wadi Sikait. The first location (Sikait-1) lies at the upper stream of Wadi Sikait, while the second location (Sikait-2) occurs west the bend of Wadi Sikait (Fig. 1). The origin of the metamorphosed sandstone rocks are sandstones which may be subjected to heat with or without pressure

Sikait-1 is the largest outcrop of metamorphosed sandstone (1.4 km in length and ranged in width from 120 m to 300 m) with low to medium peaks, elongated in NW-SE direction. These rocks are ranged in color from pale white to milky white and characterized by mylonitization and many types of alterations (silicification, Fe-Mn oxy-hydroxides, sericitization and kaolinitization). Visible mineralization occurs along the fault zones and it can see by naked eyes.

Sikait-2 covers a small area from the studied metamorphosed sandstone, where its length is about 450 m and maximum width about 230 m, forming low terrain and highly sheared rocks. It is characterized by silicification alteration. Many mineralizations are associated with quartz veins rich in fluorite and wolframite along the fault zones at the west side of this location.

Metamorphosed sandstones are greywackes according to the petrographically study and characterized by hematitizations and manganese oxides along fractures, generally uniform in texture and composed from fused quartz grains. Semi-angular and elongated rock fragments of older rocks are enclosed in metamorphosed sandstones.

Lamprophyre dykes

Lamprophyre dykes are compact, black or dark black in color, altered, fine –grained, discontinuous and vary in thickness from 0.5 to 2 m and up to 1.4 km in length. These dykes cut both of metamorphosed sandstones and porphyritic biotite granite. The trends of these dykes are concordant with the main structural trends affected in the study area, so that they run in NW-SE, NNE-SSW and N-S. The lamprophyre dykes are considered as the probable traps of uranium and other mineralization.

Analytical Technique

Fourteen metamorphosed sandstone rock samples were collected from Sikait-1 (8 samples) and Sikait-2 (6 samples). These samples were prepared for γ-ray spectrometric analyses by HPGe detector system. The studied samples were measured by using the HPGe detector. This detector has a relative efficiency of about 50% of the 3″×3″ NaI(Tl) crystal efficiency, resolution of 1.90 keV and peak/Compton ratio of 69.9:1 at the 1.33 MeV gamma transition of ^{60}Co. It is coupled to conventional electronics connected to a multichannel analyzer card (MCA) installed in a PC computer. The efficiency calibration was performed by using three well-known reference materials obtained from the International Atomic Energy Agency for U, Th and K activity measurements: RGU-1, RGTh-1 and RGK-1 (IAEA, 1987, Anjos *et al*., 2005). Absolute efficiency calibration of the gamma spectrometry system was carried out using the radionuclide specific efficiency method in order to reduce the uncertainty in gamma-ray intensities, as well as the influence of coincidence summation and self-absorption effects of the emitting gamma photons (Stoulos *et al*., 2003).

The primordial ^{238}U is the most abundant isotope of U (99.27 %) and the initial member of the ^{238}U-decay chain with a long half-life time (4.4683 Ga). It decays to ^{234}Th with the emission of the α-particle. Through two consecutive β- transitions, ^{234}Th decays to ^{234}Pa (half-lives of 24.10 days and 6.69 h, respectively) and to ^{234}U, with the half-life time of 245,250 years, which decays to ^{230}Th (Pękala *et al*., 2010). Uranium-238 activity was determined indirectly from the gamma rays emitted by its daughter products (^{234}Th and ^{234m}Pa) whose activities are determined from the 63.3 and 1001 keV photopeaks, respectively (Sutherland and de Jong, 1990). The ^{234}U activity was determined directly from the gamma rays emitted from this nuclide at energies of 53.2 and 120.9 keV (Yokoyama *et al*., 2008; Yücel *et al*., 2010; Ramebäck *et al*., 2010). For the measurement of the ^{230}Th activity, the γ-ray emission at 67.7 keV is used (Simpson and Grün, 1998).

The specific activity of ^{226}Ra was measured using the 186.1 keV from its own gamma-ray (after the subtraction of the 185.7 keV of ^{235}U). The specific activity of ^{214}Pb was measured using the 241.9, 295.2 keV and 351.9 keV while the specific activities of ^{214}Bi and ^{210}Pb were measured using 609.3 and 46.5 keV, respectively.

The uranium-235 activity was determined directly by its gamma ray peaks; 143.8, 163.4, 185.7, and 205.3 keV (Yücel *et al*., 1998; Pöllänen *et al*., 2003; Ramebäck *et al*., 2010). The specific activity of ^{232}Th was measured using the 338.4 keV and 911.2 keV from ^{228}Ac and 583 keV and 2614.4 keV from ^{208}Tl. The specific activity of ^{40}K was measured directly by its own gamma-ray at 1460.8 keV.

RESULTS AND DISCUSSION

The measured isotopic compositions and the isotopic ratios of the samples are shown in Table 1. Isochron-derived authigenic ^{230}Th/^{234}U and ^{234}U/^{238}U values and calculated ages are summarized in Table 2. Ages and errors have been calculated using the Isoplot program of Ludwig (1994).

The ^{238}U concentrations of the analysed samples vary from 8.24 to 40.13 ppm in Sikait-1 and from 7.93 to 19.73 ppm in Sikait-2, while the ^{232}Th concentrations vary from 2.84 to 90.84 ppm in Sikait-1 and from 9.98 to 51.54 ppm in Sikait-2.

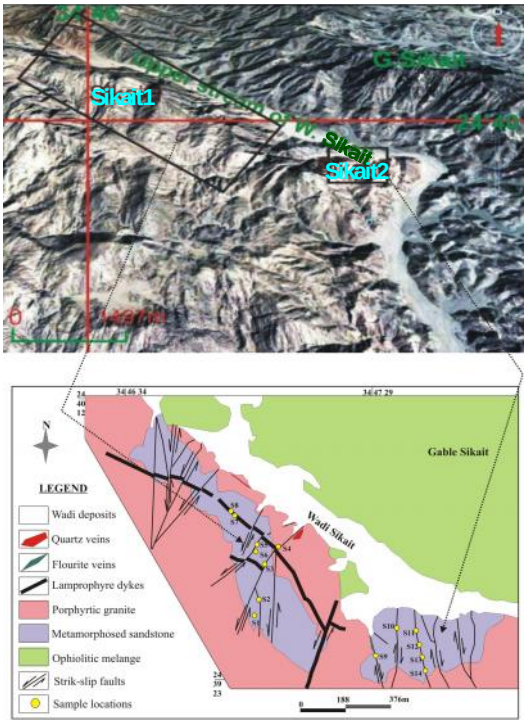

Fig. 1 Location map of Sikait-1 and Sikait-2 and their detailed geologic map (modified after Ibrahim *et al*., 2010).

According to Clark *et al*. (1966), Th:U ratio in igneous rocks is about 3.5 or 4:1. This ratio depends mainly on the content of U (mobile element) so, Th:U ratio is important for U exploration through the determination of U-rich areas. Therefore, in granites, U enrichment (leach in of U) can be indicated by low ratio (< 3.5), while U depletion [leach out of U (mobilization) or initially U poor source] is indicated by high ratio (> 3.5). In the present study, Th:U ratio ranges between 0.12 and 3.18 in Sikait-1 and between 1.21 and 2.73 in Sikait-2 [all lower than Clark value indicate enrichment of U except one sample (S2) which is close to Clark value] which are shown in figure (2).

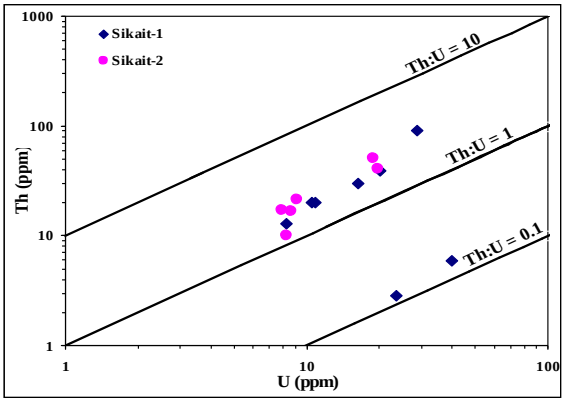

Fig. 2 The relationship between U and Th for the studied samples

Activity Ratios

Uranium-series disequilibrium can potentially provide an important tool for tracing migration of uranium series radionuclides and groundwaters from different aquifer conditions and, thus, has extensively been applied to the study of environmental, marine and earth sciences (Osmond and Ivanovich, 1992). In closed geological systems the nuclides ^{238}U–^{234}U–^{230}Th attain radioactive equilibrium after 1.7 Ma (Gascoyne *et al*., 2002), i.e., respective activity ratios (AR) ^{234}U/^{238}U, ^{230}Th/^{234}U and ^{230}Th/^{238}U all equal unity.

If the systems are exposed to weathering and groundwater circulation, the different physico-chemical conditions affecting ^{238}U and ^{234}U will result in their fractionation and, thus, the respective activity ratios will therefore be greater or less than unity. The isotopic variation of U results from selective leaching of ^{234}U itself and the direct α-recoil transfer of a ^{234}U precursor (^{234}Th). ^{234}U atoms are more susceptible to leaching than ^{238}U atoms as a result of α-recoil within the mineral lattice. The preferential leaching of ^{234}U will result in ^{234}U/^{238}U less than 1.0 in the weathering mineral. This results in the enrichment of ^{234}U in groundwater and a ^{234}U depletion in the mineral. An additional mechanism is the process of daughter product emplacement from pore waters containing dissolved ^{234}U and ^{238}U, resulting in rocks that are enriched in ^{234}U and ^{230}Th relative to ^{238}U in reducing environments. Thus, using the measured daughter/parent activity ratios ^{234}U/^{238}U, ^{230}Th/^{234}U and ^{226}Ra/^{230}Th, U migration over various time-scales of 1.0 Ma, 300 ka and 6 ka, respectively, can be evaluated (Min *et al*., 2005; Dawood, 2010).

Generally, the weathered rocks deviate from secular equilibrium due to the differences in radionuclides mobility during weathering processes. This relative mobility is believed to be ^{234}U> ^{238}U> ^{230}Th, and consequently the weathered rocks are estimated to have ^{234}U/^{238}U<1 and ^{230}Th/^{238}U>1. The extent of disequilibrium depends on both the intensity and age of weathering processes. Chemical processes and the alpha-recoil

effects are the main factors responsible for the uranium-series disequilibrium. It is reasonable to determine the time of the disequilibrium event by measuring the extent to which the isotope system has returned to the state of secular equilibrium (Dawood, 2009).

secondary uranium ore are characterized by $^{234}U/^{238}U$ >1 and $^{230}Th/^{234}U$ <1. This indicates relatively recent precipitation of uranium from water with $^{234}U/^{238}U$ >1. This result is similar to six samples in present study [samples (S1, S2 and S3) in Sikait-1 and samples (S10, S12 and S13) in Sikait-2, Fig. 3a] and also similar to the cases studied by Levinson *et al*. (1984) and Osmond *et al*. (1999).

Table 1 Specific activity (Bq kg^{-1}) of radionuclides and different activity ratios for studied samples

Nuclide	Sikait-1															
	S1		S2		S3		S4		S5		S6		S7		S8	
^{238}U series																
^{234Th}	203.53	± 9.34	357.83	± 19.78	507.79	± 19.57	251.01	± 16.39	103.45	± 4.01	136.03	± 5.09	132.05	± 7.56	292.29	± 12.95
^{234m}Pa	201.57	± 45.10	350.94	± 59.97	487.48	± 104.26	251.57	± 55.96	100.97	± 16.99	133.05	± 21.99	129.47	± 27.94	293.30	± 52.62
Average	**202.55**	**± 27.22**	**354.38**	**± 39.87**	**497.63**	**± 61.92**	**251.29**	**± 36.17**	**102.21**	**± 10.50**	**134.54**	**± 13.54**	**130.76**	**± 17.75**	**292.79**	**± 32.79**
^{234}U	259.81	± 56.79	375.29	± 84.18	610.87	± 112.41	215.59	± 64.26	80.25	±19.21	127.72	± 20.12	100.09	± 21.44	267.32	± 35.56
^{230Th}	191.26	± 73.92	240.35	± 66.99	461.22	± 100.04	201.99	± 49.94	101.49	± 38.88	103.17	± 43.23	128.14	± 19.73	253.81	± 46.54
^{226}Ra	165.64	± 7.33	624.07	± 18.73	524.39	± 17.86	170.86	± 8.32	100.17	± 3.18	104.70	± 3.29	106.06	± 2.84	205.85	± 6.43
^{214}Pb	127.88	± 2.64	335.63	± 4.87	453.44	± 7.58	153.55	± 3.53	96.47	± 1.35	99.68	± 1.28	96.72	± 1.32	202.23	± 2.87
^{214}Bi	127.12	± 2.57	333.89	± 4.66	449.63	± 7.24	151.72	± 3.20	96.11	± 1.31	99.56	± 1.24	96.55	± 1.24	201.93	± 2.69
^{210}Pb	134.46	± 8.31	329.01	±13.79	422.66	± 18.25	130.27	± 10.50	100.89	± 3.43	104.41	± 3.54	90.47	± 3.76	171.47	± 6.28
^{232}Th series																
^{228}Ac	123.49	± 4.01	372.05	± 7.70	23.99	± 3.96	158.64	± 5.51	52.33	± 1.73	81.60	± 1.94	82.20	± 1.99	11.93	± 1.85
^{208}Tl	118.14	± 3.67	361.95	± 7.40	23.27	± 2.64	155.60	± 4.99	52.16	± 1.42	80.29	± 1.72	80.46	± 1.83	10.99	± 0.93
Average	**120.81**	**± 3.84**	**367.00**	**± 7.55**	**23.63**	**± 3.30**	**157.12**	**± 5.25**	**52.24**	**± 1.58**	**80.95**	**± 1.83**	**81.33**	**± 1.91**	**11.46**	**± 1.39**
^{235}U	**9.31**	**± 0.75**	**16.36**	**± 2.75**	**22.86**	**± 1.68**	**11.58**	**± 2.35**	**4.72**	**± 0.59**	**6.25**	**± 0.75**	**6.04**	**± 0.83**	**13.37**	**± 0.81**
^{40}K	**1690.27**	**± 22.75**	**1773.38**	**± 27.59**	**694.16**	**± 22.44**	**1263.17**	**± 23.91**	**970.42**	**± 10.28**	**1136.89**	**± 10.77**	**1161.38**	**± 10.93**	**730.20**	**± 13.50**
$^{238}U/^{235}U$	21.76	± 4.69	21.67	± 6.09	21.76	± 4.31	21.71	± 7.53	21.67	± 4.94	21.54	± 4.74	21.64	± 5.91	21.90	± 3.77
$^{234}U/^{235}U$	27.92	± 8.37	22.94	± 9.01	26.72	± 6.88	18.62	± 9.33	17.01	± 6.20	20.45	± 5.67	16.56	± 5.82	19.99	± 3.87
$^{234}U/^{238}U$	1.28	± 0.45	1.06	± 0.36	1.23	± 0.38	0.86	± 0.38	0.79	± 0.27	0.95	± 0.25	0.77	± 0.27	0.91	± 0.22
$^{226}Ra/^{238}U$	0.82	± 0.15	1.76	± 0.25	1.05	± 0.17	0.68	± 0.13	0.98	± 0.13	0.78	± 0.10	0.81	± 0.13	0.70	± 0.10
$^{230Th}/^{238}U$	0.94	± 0.49	0.68	± 0.27	0.93	± 0.32	0.80	± 0.31	0.99	± 0.48	0.77	± 0.40	0.98	± 0.28	0.87	± 0.26
$^{230Th}/^{234}U$	0.74	± 0.45	0.64	± 0.32	0.76	± 0.30	0.94	± 0.51	1.26	± 0.79	0.81	± 0.47	1.28	± 0.47	0.95	± 0.30
$^{226}Ra/^{230}Th$	0.87	± 0.37	2.60	± 0.80	1.14	± 0.29	0.85	± 0.25	0.99	± 0.41	1.01	± 0.46	0.83	± 0.15	0.81	± 0.17
$^{210}Pb/^{226}Ra$	0.81	± 0.09	0.53	± 0.04	0.81	± 0.06	0.76	± 0.10	1.01	± 0.07	1.00	± 0.07	0.85	± 0.06	0.83	± 0.06
U (ppm)	16.33	± 2.20	28.58	± 3.22	40.13	± 4.99	20.27	± 2.92	8.24	± 0.85	10.85	± 1.09	10.55	± 1.43	23.61	± 2.64
Th (ppm)	29.90	± 0.95	90.84	± 1.87	5.85	± 0.82	38.89	± 1.30	12.93	± 0.39	20.04	± 0.45	20.13	± 0.47	2.84	± 0.34
K (%)	5.40	± 0.07	5.67	±0.09	2.22	± 0.07	4.04	± 0.08	3.10	± 0.03	3.63	± 0.03	3.71	± 0.03	2.33	± 0.04
Th/U	1.83	± 0.30	3.18	± 0.42	0.15	± 0.04	1.92	± 0.34	1.57	± 0.21	1.85	± 0.23	1.91	± 0.30	0.12	± 0.03

Table 1 Continue

Nuclide	Sikait-2											
	S9		S10		S11		S12		S13		S14	
^{238}U series												
^{234Th}	105.42	± 4.00	104.31	± 6.11	112.41	± 6.77	235.56	± 10.77	245.07	± 10.57	98.87	± 3.85
^{234m}Pa	107.40	± 15.40	101.03	± 18.62	112.38	± 18.12	233.13	± 42.12	244.22	± 45.73	97.73	± 22.80
Average	**106.41**	**± 9.70**	**102.67**	**± 12.37**	**112.40**	**± 12.45**	**234.35**	**± 26.45**	**244.64**	**± 28.15**	**98.30**	**± 13.33**
^{234}U	71.32	± 13.48	114.24	± 17.21	91.83	± 25.33	385.93	± 96.31	337.07	±105.60	87.46	± 36.74
^{230Th}	92.89	± 24.33	100.43	± 36.21	101.71	± 39.48	164.58	± 60.91	237.23	± 65.56	70.23	± 37.79
^{226}Ra	88.17	± 2.57	108.54	± 3.04	97.18	± 2.81	142.85	± 5.77	158.21	± 7.24	79.47	± 2.40
^{214}Pb	86.77	± 1.23	100.60	± 1.30	95.60	± 1.29	135.40	± 2.71	135.78	± 2.95	78.79	± 1.15
^{214}Bi	84.04	± 1.33	100.04	± 1.25	95.44	± 1.16	134.43	± 2.49	134.14	± 2.74	78.76	± 1.13
^{210}Pb	90.53	± 2.87	93.37	± 3.16	95.20	± 4.39	112.64	± 8.43	122.01	± 9.43	77.01	± 3.66
^{232}Th series												
^{228}Ac	67.81	± 1.78	41.32	± 1.49	87.55	± 1.98	209.43	± 4.86	165.67	± 5.04	69.69	± 2.01
^{208}Tl	67.03	± 1.57	39.35	± 1.19	87.41	± 1.72	207.00	± 4.76	165.03	± 4.59	69.27	± 1.66
Average	**67.42**	**± 1.68**	**40.34**	**± 1.34**	**87.48**	**± 1.85**	**208.22**	**± 4.81**	**165.35**	**± 4.82**	**69.48**	**± 1.84**
^{235}U	**4.87**	**± 0.53**	**4.68**	**± 0.38**	**5.15**	**± 0.35**	**10.77**	**± 2.07**	**11.24**	**± 1.48**	**4.63**	**± 0.51**
^{40}K	**845.18**	**± 9.40**	**738.15**	**± 8.90**	**754.03**	**± 8.61**	**238.71**	**± 8.38**	**409.34**	**± 12.44**	**921.29**	**± 9.69**
$^{238}U/^{235}U$	21.87	± 4.38	21.94	± 4.42	21.84	± 3.92	21.75	± 6.63	21.76	± 5.36	21.25	± 5.23
$^{234}U/^{235}U$	14.66	± 4.37	24.41	± 5.65	17.84	± 6.15	35.82	± 15.82	29.98	± 13.33	18.91	±10.03
$^{234}U/^{238}U$	0.67	± 0.19	1.11	± 0.30	0.82	± 0.32	1.65	± 0.60	1.38	± 0.59	0.89	± 0.49
$^{226}Ra/^{238}U$	0.83	± 0.10	1.06	± 0.16	0.86	± 0.12	0.61	± 0.09	0.65	± 0.10	0.81	± 0.13
$^{230}Th/^{238}U$	0.87	± 0.31	0.98	± 0.47	0.90	± 0.45	0.70	± 0.34	0.97	± 0.38	0.71	± 0.48
$^{230}Th/^{234}U$	1.30	± 0.59	0.88	± 0.45	1.11	± 0.74	0.43	± 0.26	0.70	± 0.42	0.80	± 0.77
$^{226}Ra/^{230}Th$	0.95	± 0.28	1.08	± 0.42	0.96	± 0.40	0.87	± 0.36	0.67	± 0.21	1.13	± 0.64
$^{210}Pb/^{226}Ra$	1.03	± 0.06	0.86	± 0.05	0.98	± 0.07	0.79	± 0.09	0.77	± 0.09	0.97	± 0.08
U (ppm)	8.58	± 0.78	8.28	± 1.00	9.06	± 1.00	18.90	± 2.13	19.73	± 2.27	7.93	± 1.07
Th (ppm)	16.69	± 0.41	9.98	± 0.33	21.65	± 0.46	51.54	± 1.19	40.93	± 1.19	17.20	± 0.45
K (%)	2.70	± 0.03	2.36	± 0.03	2.41	± 0.03	0.76	± 0.03	1.31	± 0.04	2.94	± 0.03
Th/ U	1.94	± 0.23	1.21	± 0.19	2.39	± 0.32	2.73	± 0.37	2.07	± 0.30	2.17	± 0.35

The activity ratios $^{234}U/^{238}U$ and $^{230}Th/^{234}U$ for some samples display values out of equilibrium. The activity ratios of

The removal of uranium from granitic rocks is generally characterized by $^{234}U/^{238}U \leq 1$ and $^{230}Th/^{234}U>1$ (Latham and

Schwarcz, 1987; Dawood, 2001) which similar to four metamorphosed sandstone samples in present study [samples (S5 and S7) in Sikait-1 and samples (S9 and S11) in Sikait-2, Fig. 3a]. The essential reason for these ratios is that groundwater leaches ^{234}U preferentially to ^{238}U and removes both uranium isotopes relative to ^{230}Th.

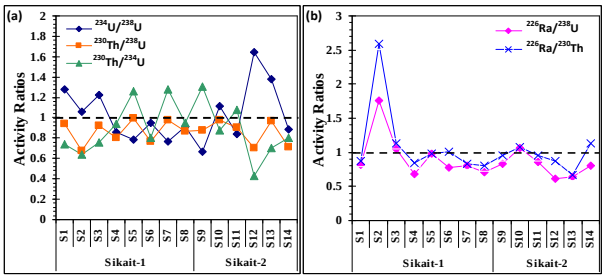

Fig. 3 Variations of the (a) $^{234}U/^{238}U$, $^{230}Th/^{238}U$ and $^{230}Th/^{234}U$ and (b) $^{226}Ra/^{238}U$ and $^{226}Ra/^{230}Th$ activity ratios in Sikait-1 and Sikait-2 samples. The equilibrium state (activity ratio=1.00) is shown with the dashed lines.

The behaviour of ^{226}Ra is markedly different between studied samples, as shown by the ($^{226}Ra/^{238}U$) or ($^{226}Ra/^{230}Th$) ratios. While U is immobile in a reducing environment, and becomes soluble only under oxidising conditions, Ra can easily be mobilised under reducing conditions but is readily adsorbed onto minerals formed in oxidised zones, like iron hydroxides. Conversely, Ra is sometimes adsorbed onto clay minerals in non oxidised zones. This suggests that the redox conditions at the time of fluid circulation are not the only parameter affecting Ra mobility. The mineralogy of the rocks resulting from past alteration events probably plays an important role together with the chemical composition and redox potential of the fluids (Condomines *et al*., 2007).

The $^{226}Ra/^{238}U$ ratios are lower than unity in most samples (samples S3, S5 and S10 are in ^{226}Ra-^{238}U radioactive equilibrium), whereas they are higher than unity in one sample (S2) as shown in figure (3b). It is usually explained by the contrasted chemical properties of U and Ra. However, if secondary U minerals are present in oxidised zones, Ra might also be leached from these minerals (a process enhanced by alpha-recoil effects), resulting in a net Ra deficit even if some Ra is adsorbed onto iron-hydroxides.

There is a contrast in behaviour between samples. ^{226}Ra is in equilibrium with ^{230}Th in five samples [(S5 and S6) from Sikait-1 and (S9, S10 and S11) from Sikait-2], whereas ^{226}Ra is in excess in three samples [(S2 and S3) from Sikait-1 and (S14) from Sikait-2] as shown in figure (3b). This could be due to a ^{226}Ra gain resulting from recoil-implanted ^{226}Ra atoms from decay of ^{230}Th atoms and Ra readily adsorbed onto minerals formed in oxidised zones.

If Ra redistribution is caused by an instantaneous chemical process, it must have occurred during the last 8000 years, which is the time needed to reach radioactive equilibrium between ^{226}Ra and ^{230}Th. A more continuous redistribution process could have started earlier, but should still have been active during the last 8000 years (Condomines *et al*., 2007).

Four of Sikait-1 samples (S1, S4, S7 and S8) and two of Sikait-2 samples (S12 and S13) have ($^{226}Ra/^{230}Th$) ratios lower than unity, implying preferential removal of ^{226}Ra (Fig. 3b).

Measured $^{234}U/^{238}U$, $^{230}Th/^{238}U$, $^{230}Th/^{234}U$ and $^{226}Ra/^{230}Th$ for eight metamorphosed sandstone samples from Sikait-1 vary from 0.77 to 1.28, from 0.68 to 0.99, from 0.64 to 1.28 and from 0.81 to 2.60, respectively.

For six metamorphosed sandstone samples collected from Sikait-2, the four ratios range from 0.67 to 1.65, from 0.70 to 0.98, from 0.43 to 1.30, and from 0.67 to 1.13, respectively.

In a plot of $^{234}U/^{238}U$ versus $^{230}Th/^{238}U$ as shown in figure 4, the pathways of return to equilibrium for solid phases are shown for two cases: accumulation of U ($^{230}Th/^{238}U$ decrease) and leaching of U ($^{230}Th/^{238}U$ increase) (Thiel *et al*., 1983; Brantley *et al*., 2008). The presence of data points in the forbidden zones may be explained as a result of continuous and contrasting U mobilization processes (Chabaux *et al*., 2003). According to judging standards, activity ratios between 0.90 and 1.10 are referred as secular equilibrium within the conservative (10 %) analytical error for the samples (Min *et al*., 2005). It is supported by the Thiel diagram (Fig. 4), in which the samples that plot into the boxed-in area are considered near or at secular radioactive equilibrium. All cases of U leaching are characterized by ($^{234}U/^{238}U$) AR < 1 and all cases of U accumulation are distinguished by the relation ($^{234}U/^{238}U$) AR > 1 (Thiel *et al*., 1983).

As show in figure 4, both the two locations [Sikait-1 and Sikait-2] show leaching [(S5 and S7) from Sikait-1 and (S9 and S11) from Sikait-2] and accumulation [(S1, S2 and S3) from Sikait-1 and (S10, S12 and S13) from Sikait-2] of uranium which are confirmed by the samples located in forbidden zone [(S4, S6 and S8) from Sikait-1 and (S14) from Sikait-2].

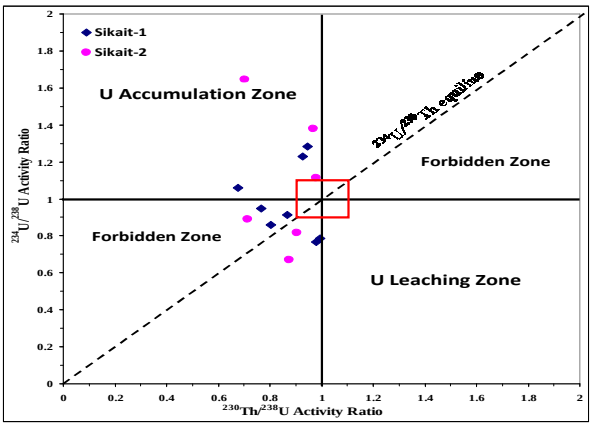

Fig 4 Thiel diagram showing the evolution of $^{234}U/^{238}U$ versus $^{230}Th/^{238}U$ activity ratios.

Plots of the samples deviating from secular equilibrium, i.e., larger than 1.10 or less than 0.90 for $^{234}U/^{238}U$, $^{230}Th/^{238}U$, $^{230}Th/^{234}U$ and $^{226}Ra/^{230}Th$, fall into the forbidden region in the Thiel diagram (Fig. 4). The forbidden zone is a complex geochemical region where the systems can be identified as having suffered complicated U migration. A complex leaching and accumulation of uranium might take place for those

samples in forbidden zone. The samples fall into forbidden zone are (S4, S6 and S8) from Sikait-1 and (S14) from Sikait-2. The ARs of $^{238}U/^{235}U$ for all studied samples are ranging between 21.25 (sample S14 from Sikait-2) and 21.94 (sample S10 from Sikait-2) which reflect little deviation from the natural ratio (21.7) and the alteration process affect this ratio (Fig. 5a).

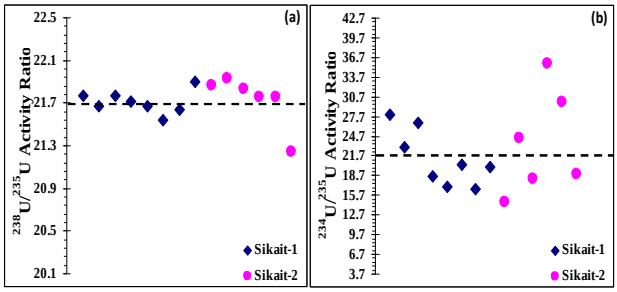

Fig. 5 Variations of the 238U/235U and 234U/235U activity ratios in Sikait-1 and Sikait-2 samples. The certified value of 238U/235U activity ratio is 21.7, which is shown with the dashed lines

Although significant variations in the $^{238}U/^{235}U$ ratio are a recent discovery, much larger variations in the $^{234}U/^{235}U$ ratio in the terrestrial variations have long been observed. Specifically, the increased mobility of ^{234}U relative to other U isotopes reflects production from ^{238}U by α-decay and subsequent emplacement in crystal sites damaged by α-recoil. Aqueous weathering of materials containing U results in preferential leaching of ^{234}U from these α-damaged crystal sites (Brennecka *et al*., 2010). In reverse to the values of $^{238}U/^{235}U$ ratios, the $^{234}U/^{235}U$ ratios in the Sikait-1 samples range between 16.56 and 27.92 while in the Sikait-2 samples range between 14.66 and 35.82 which means a uranium-234 leaching out and in due to alteration processes (Fig. 5b).

Uranium-series dating

Table 2 shows the calculated ages of deposition of the studied metamorphosed sandstone rock samples in Sikait-1 and Sikait-2.

The existence of radioactive disequilibria among nuclides in the decay series is an indication of recent fractionation events, usually related to gain or loss of the more mobile nuclides (Condomines *et al*., 2007). Fontes *et al* (1992) reported that either gain or loss of U may occur in lacustrine samples due to changing redox conditions. Uranium gain causes the calculated U-series date to be younger and U loss causes the date to be older than the true age (Szabo *et al*., 1995). The understanding of the U-migration process is significant for the calculation of U-series dating results (Simpson and Grün, 1998).

Samples (S5 and S7) from Sikait-1 and (S9 and S11) from Sikait-2 severe differential isotopic fractionation, especially ^{230}Th fractionation. These samples have an excess of ^{230}Th relative to ^{234}U and the activity ratio $^{230}Th/^{234}U$ is more than one and therefore being undatable because, in this case, the activity of the daughter exceeds the secular equilibrium with its parent. Consequently, the isochrons are unreliable.

The uranium series age of 80,000–140,000 yr for the secondary uranium deposits from the central Eastern Desert of Egypt has been reported by Osmond *et al*. (1999). Dawood (2001) found that the $^{230}Th/^{234}U$ age of secondary uranium ore from the south Eastern Desert of Egypt varies from 50,000 to 159,000 yr.

As shown in table 2, the age of uranium deposition for Sikait-1 samples ranges from 109,600 to 460,100 yr while for Sikait-2 samples ranges from 57,970 to 211,800 yr.

The $^{230}Th/^{232}Th$ activity ratios range between 0.65 and 22.15 for Sikait-1 samples and between 0.79 and 2.49 for Sikait-2 samples which are smaller than 20 except one sample (S8), indicating a contamination of the samples by detrital ^{230}Th.

Indeed, the studied samples are all characterised by low $^{230}Th/^{232}Th$ ratios indicating contamination by detrital materials except one sample (S8). Therefore, the ages presented in Table 2 are overestimated and represent maximum ages.

Table 2 Specific activities of ^{238}U, ^{234}U and ^{230}Th, isotopic activity ratios and ages of deposition for Sikait-1 and Sikait-2 samples.

Sample No.	Sample Location	^{238}U (Bq/kg)	^{234}U (Bq/kg)	^{230}Th (Bq/kg)	^{232}Th (Bq/kg)	Activity Ratios $^{234}U/^{238}U$	$^{230}Th/^{232}Th$	$^{230}Th/^{234}U$	Age (ka)[1]	Age (ka)[2]
S1	Sikait-1	202.55 ± 27.22	259.81 ± 56.79	191.26 ± 73.92	120.81 ± 3.84	1.28 ± 0.45	1.58 ± 0.66	0.74 ± 0.45	134.3 + 0.77 - 2.70	127.4 + 0.79 - 2.78
S2		354.38 ± 39.87	375.29 ± 84.18	240.35 ± 66.99	367.00 ± 7.55	1.06 ± 0.36	0.65 ± 0.20	0.64 ± 0.32	109.6 + 0.95 - 2.65	97.17 + 1.02 - 2.85
S3		497.63 ± 61.92	610.87 ± 112.41	461.22 ± 100.04	23.63 ± 3.30	1.23 ± 0.38	19.52 ± 6.96	0.76 ± 0.30	142.6 + 0.89 - 2.00	141.9 + 0.89 - 2.01
S4		251.29 ± 36.17	215.59 ± 64.26	201.99 ± 49.94	157.12 ± 5.25	0.86 ± 0.38	1.29 ± 0.36	0.94 ± 0.51	328.8 + 0.60 - 1.84	341.2 + 0.62 - 1.91
S6		134.54 ± 13.54	127.72 ± 20.12	103.17 ± 43.23	80.95 ± 1.83	0.95 ± 0.25	1.27 ± 0.56	0.81 ± 0.47	185.2 + 0.73 - 2.47	168 + 0.76 - 2.56
S8		292.79 ± 32.79	267.32 ± 35.56	253.81 ± 46.54	11.46 ± 1.39	0.91 ± 0.22	22.15 ± 6.75	0.95 ± 0.30	460.1 + 0.77 - 1.46	441.9 +0.77 - 1.46
S10		102.67 ± 12.37	114.24 ± 17.21	100.43 ± 36.21	40.34 ± 1.34	1.11 ± 0.30	2.49 ± 0.98	0.88 ± 0.45	211.8 + 0.71 - 2.05	201.1 + 0.72 - 2.09
S12	Sikait-2	234.35 ± 26.45	385.93 ± 96.31	164.58 ± 60.91	208.22 ± 4.81	1.65 ± 0.60	0.79 ± 0.31	0.43 ± 0.26	57.97 + 1.28 - 4.65	53.71 + 1.36 - 4.94
S13		244.64 ± 28.15	337.07 ± 105.60	237.23 ± 65.56	165.35 ± 4.82	1.38 ± 0.59	1.43 ± 0.44	0.70 ± 0.42	122.2 + 0.76 - 2.58	115.5 + 0.79 - 2.66
S14		98.30 ± 13.33	87.46 ± 36.74	70.23 ± 37.79	69.48 ± 1.84	0.89 ± 0.49	1.01 ± 0.57	0.80 ± 0.77	190.4 + 0.47 - 3.83	167.7 + 0.49 - 4.01

[1] The uncorrected age for samples.
[2] The corrected age after subtraction detrital ^{230}Th for samples.

So the plot of the $^{230}Th/^{232}Th$ activity ratios versus the $^{234}U/^{232}Th$ activity ratios is used for determination of the global detrital correction factor $^{230}Th/^{232}Th$. This factor is then used to correct each sample separately (Schirrmeister *et al*., 2002).

The isochron-corrected ages of five samples (S1, S2, S3, S4 and S6) were corrected with a $^{230}Th/^{232}Th$ ratio of 0.0465 as shown in figure 6. By using equation (2), calculated the actual radiogenic ^{230}Th and age of studied samples.

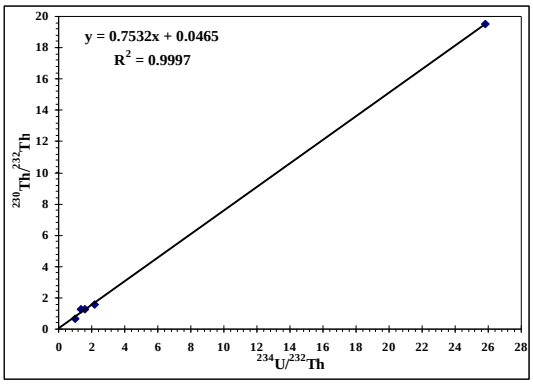

Fig. 6 $^{230}Th/^{232}Th$ vs $^{234}U/^{232}Th$ activity ratio isochron diagram

The plot of the $^{238}U/^{234}U$ activity ratios versus the detritus-corrected $^{230}Th/^{234}U$ activity ratios is used to verify closed-system conditions (Fig. 7). Table 2 and figure 7 show the age of uranium deposition after subtraction the detrital ^{230}Th. The corrected age for Sikait-1 samples vary from 97.17 to 441.9 kyr while for Sikait-2 samples vary from 53.71 to 201.1 kyr.

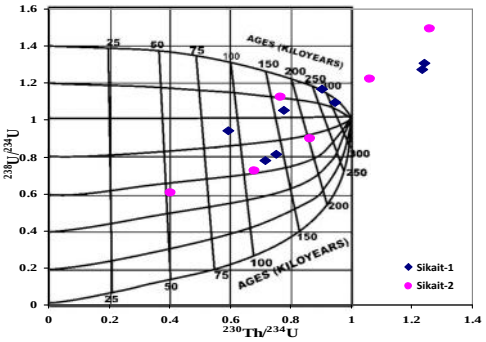

Fig. 7 Cross plot of isotopic ratios for metamorphosed sandstone rock samples from the study area (After Osmond *et al*., 1999).

Specific activities for some of the metamorphosed sandstone samples [(S5 and S7) from Sikait-1 and (S9 and S11) from Sikait-2] are $^{238}U > ^{234}U < ^{230}Th > ^{226}Ra$, indicating that leaching of daughter products has taken place or that uranium has migrated to its present location in the last 1.0 Ma, which is less than the time required by the daughter products to reach approximate equilibrium therefore in this case these samples being undatable because, the activity of the daughter exceeds the secular equilibrium with its parent.

Specific activities of the others [(S1, S2 and S3) from Sikait-1 and (S10, S12 and S13) from Sikait-2] are $^{238}U < ^{234}U > ^{230}Th > ^{226}Ra$ or $^{238}U < ^{234}U > ^{230}Th < ^{226}Ra$, indicating recent accumulation of uranium (Osmond and Ivanovich, 1992). The $^{234}U/^{238}U$ for these samples is mostly greater than 1.0 due to enrichment of ^{234}U and ^{230}Th relative to ^{238}U in a reducing environment.

CONCLUSION

The detailed field study of the studied area revealed that the metamorphosed sandstones occur in two location at Wadi Sikait [Sikait-1 and Sikait-2]. Th:U ratio ranges between 0.12 and 3.18 in Sikait-1 and between 1.21 and 2.73 in Sikait-2 indicating U enrichment except one sample (S2) which is close to the natural value. The activity ratios of secondary uranium ore are characterized by $^{234}U/^{238}U > 1$ and $^{230}Th/^{234}U < 1$ as in samples (S1, S2 and S3) in Sikait-1 and samples (S10, S12 and S13). This indicates relatively recent precipitation of uranium from water with $^{234}U/^{238}U > 1$. $^{234}U/^{238}U \leq 1$ and $^{230}Th/^{234}U > 1$ which in four metamorphosed sandstone samples (S5 and S7) in Sikait-1 and samples (S9 and S11) in Sikait-2. The essential reason for these ratios is that groundwater leaches ^{234}U preferentially to ^{238}U and removes both uranium isotopes relative to ^{230}Th. $^{230}Th/^{238}U$ activity ratios for all studied samples are less than unity whereas seven of them are close to ^{230}Th-^{238}U equilibrium [samples (S1, S3, S5 and S7) in Sikait-1 and samples (S10, S11 and S13) in Sikait-2]. These results indicate that all ^{230}Th are produced by in situ decay of ^{234}U and there is no allogenic or initial ^{230}Th which are confirmed by the results of the ^{232}Th:^{238}U concentration ratios mentioned before. So we can conclude that the uranium content in the studied area is recently deposited.

The $^{226}Ra/^{238}U$ ratios are lower than unity in most samples (samples S3, S5 and S10 are in ^{226}Ra-^{238}U radioactive equilibrium), whereas they are higher than unity in one sample (S2) which is usually explained by the contrasted chemical properties of U and Ra. However, if secondary U minerals are present in oxidised zones, Ra might also be leached from these minerals (a process enhanced by alpha-recoil effects), resulting in a net Ra deficit even if some Ra is adsorbed onto iron-hydroxides. ^{226}Ra is in equilibrium with ^{230}Th in five samples [(S5 and S6) from Sikait-1 and (S9, S10 and S11) from Sikait-2], whereas ^{226}Ra is in excess in three samples [(S2 and S3) from Sikait-1 and (S14) from Sikait-2]. This could be due to a ^{226}Ra gain resulting from recoil-implanted ^{226}Ra atoms from decay of ^{230}Th atoms and Ra readily adsorbed onto minerals formed in oxidised zones. Four of Sikait-1 samples (S1, S4, S7 and S8) and two of Sikait-2 samples (S12 and S13) have ($^{226}Ra/^{230}Th$) ratios lower than unity, implying preferential removal of ^{226}Ra. If Ra redistribution is caused by an instantaneous chemical process, it must have occurred during the last 8000 years, which is the time needed to reach radioactive equilibrium between ^{226}Ra and ^{230}Th.

The ARs of $^{238}U/^{235}U$ for all studied samples are ranging between 21.25 (sample S14 from Sikait-2) and 21.94 (sample S10 from Sikait-2) which reflect little deviation from the natural ratio (21.7) and the alteration process affect this ratio. In reverse to the values of $^{238}U/^{235}U$ ratios, the $^{234}U/^{235}U$ ratios in the Sikait-1 samples range between 16.56 and 27.92 while in the Sikait-2 samples range between 14.66 and 35.82 which means a uranium-234 leaching out and in due to alteration processes.

At $^{234}U/^{238}U$ versus $^{230}Th/^{238}U$ activity ratios diagram, the two locations [Sikait-1 and Sikait-2] show leaching [(S5 and S7) from Sikait-1 and (S9 and S11) from Sikait-2] and accumulation [(S1, S2 and S3) from Sikait-1 and (S10, S12 and S13) from Sikait-2] of uranium which are confirmed by the samples located in forbidden zone.

The calculated ages of metamorphosed sandstone samples indicate major U accumulation in age ranges between 109.6 and 460.1 ky ago for Sikait-1 and between 57.97 and 211.8 ky ago for Sikait-2. The $^{230}Th/^{232}Th$ activity ratios range between 0.65 and 22.15 for Sikait-1 samples and between 0.79 and 2.49 for Sikait-2 samples which are smaller than 20 except one sample (S8), indicating a contamination of the samples by detrital ^{230}Th. So, after subtraction the detrital ^{230}Th, the corrected age for Sikait-1 samples vary from 97.17 to 441.9 kyr while for Sikait-2 samples vary from 53.71 to 201.1 kyr. These ages are conformable with U-series ages reported for secondary uranium minerals in the eastern and western deserts and indicate that there is more than one phase of uranium mineralization in the studied area.

References

Anjos, R. M., Veiga, R., Soares, T., Santos, A.M.A., Aguiar, J.G., Frascá, M.H.B.O., Brage, J.A.P., Uzêda, D., Mangia, L., Facure, A., Mosquera, B., Carvalho, C., Gomes, P.R.S., 2005. Natural radionuclide distribution in Brazilian commercial granites. Radiation Measurements, 39, 245–253.

Brantley, S.L., Kubicki, J.D., White, A.F., 2008. Kinetics of Water-Rock Interaction, Springer Science+Business Media, LLC, New York, USA, 833 p.

Brennecka, G.A., Borg, L.E., Hutcheon, I.D., Sharp, M.A., Anbar. A.D., 2010. Natural Variations in Uranium Isotope Ratios of Uranium Ore Concentrates: Understanding the $^{238}U/^{235}U$ Fractionation Mechanism. Earth and Planetary Science Letters, 291, 228–233.

Calsteren, P., Thomas, L., 2006. Uranium-series dating applications in natural environmental science. Earth-Science Reviews, 75, 155–175.

Chabaux F., Riotte J., Dequincey O., 2003. Uranium-series geochemistry: U-Th-Ra fractionation during weathering and river transport. Reviews in Mineralogy and geochemistry, 52, 533–576.

Choukri, A., Hakam, O.K., Reyss, J.L., Plaziat, J.C., 2007. Radiometrical data obtained by alpha spectrometry on unrecrystallized fossil coral samples from the Egyptian sholine of the north-western Red Sea. Radiation Measurements, 42, 271–280.

Clark, S.P.J., Peterman, Z.E., Heier, K.S., 1966. Abundances in uranium, thorium and potassium. In: Handbook of physical constants, Geol. Soc. Am., Memoir, 97, 521–541.

Condomines, M.; Loubeau, O., Patrier, P., 2007. Recent mobilization of U-series radionuclides in the Bernardan U deposit (French Massif Central). Chemical Geology., 244, 304–315.

Dawood, Y.H., 2009. Radiogenic Isotope Fractionation as an Indication for Uranium Mobility in the Granites of El Shallal Area, West Central Sinai, Egypt. JKAU; Earth Sci., 20/1, 215-238.

Dawood, Y.H., 2001. Uranium-series disequilibrium dating of secondary uranium ore from the south Eastern Desert of Egypt. Applied Radiation and Isotopes, 55, 881–887.

Dawood, Y.H., 2010. Factors Controlling Uranium and Thorium Isotopic Composition of the Streambed Sediments of the River Nile, Egypt. JAKU: Earth Sci., 21/2, 77–103.

Dawood, Y.H., Abd El-Naby, H.H., Ghaleb, B., 2014. U-series isotopic composition of kasolite associated with aplite-pegmatite at Jabal Sayid, Hijaz region, Kingdom of Saudi Arabia. Arab J Geosci, DOI 10.1007/s12517-013-0963-9.

Dawood, Y.H., Aref, M.A., Mandurah, M.H., Hakami, A., Gameil, M., 2013. Isotope geochemistry of the Miocene and Quaternary carbonate rocks in Rabigh area, Red Sea coast, Saudi Arabia. *Journal of Asian Earth Sciences*, 77, 151–162.

Fontes, J.-C., Andrews, J.N., Causse, C., Gibert, E., 1992. A comparison of radiocarbon and U/Th ages on continental carbonates. Radiocarbon, 34: 602-610.

Fowler, A., Osman, A.F., 2009. The Shait-Nugrus shear zone separating central and south Eastern Deserts, Egypt: A post-arc collision low-angle normal ductile shear zone, *Journal of African Earth Sciences*, 53, 16-32.

Fritz, H., Wallbrecher, E., Khudeir, A.A., Abu El Ela, F., Dallmeyer, R.D., 1996. Formation of Neoproterozoic metamorphic core complexes during oblique convergence (Eastern Desert, Egypt). *Journal of African Earth Science*, 23, 311–329.

Gascoyne, M., Millera, N.H., Neymarkb, L.A., 2002. Uranium-series disequilibrium in tuffs from Yucca Mountain, Nevada, as evidence of pore-fluid over the last million years. Appl. Geochem., 17, 781–795.

Geyh, M.A., 2001. Reflections on the $^{230}Th/U$ Dating of Dirty Material. *Journal on Methods and Applications of Absolute Chronology*, GEOCHRONOMETRIA, 20, 9-14.

Greiling, R.O., Kröner, A., El-Ramly, M.F., Rashwan, A.A., 1988. Structural relationships between the southern and central parts of the Eastern Desert of Egypt: details of a fold and thrust belt. In: El-Gaby, S., Greilling, R.O. (Eds.), The Pan-African belt of Northeast Africa and Adjacent Areas. Vieweg, Wiesbaden, 121–146.

IAEA, International Atomic Energy Agency, 1987. Preparation and Certification of IAEA Gamma Spectrometry Reference Materials, RGU-1, RGTh-1 and RGK-1. International Atomic Energy Agency. Report-IAEA/RL/148.

Ibrahim, M.E., Saleh, G.M., Ibrahim, W.S., 2010. Low grade metamorphosed sandstone-type uranium deposit, Wadi Sikait, South Eastern Desert, Egypt, *Journal of Geology and Mining Research*, 2(6), 129-141.

Ivanovich, M., Harmon, R.S., 1992. Uranium series Disequilibrium: Applications to Earth, Marine and Environmental Sciences. 911 pp.; Oxford (Oxford University Press).

Kaufman, A., Broecker, W.S., 1965. Comparison of ^{230}Th and ^{14}C ages for carbonate materials from Lakes

Lahontan and Bonneville. *Journal of Geophysical Research*, 70, 4039–4054.

Langmuir, D., Herman, J.S., 1980. The mobility of thorium in natural waters at low temperatures. Geochim. Cosmochim. Acta, 44, 1753–1766.

Latham, A.G., Schwarcz, H.P., 1987. On the possibility of determining rates of removal of uranium from crystalline igneous rocks using U-series disequilibria-1: a U-leach model, and its applicability to whole-rock data. Appl. Geochem., 2, 55–65.

Levinson, A.A., Bland, C.J., Dean, J.R., 1984. Uranium series disequilibrium in young surficial uranium deposits in southern British Columbia. Can. J. Earth Sci., 21, 559–566.

Ludwig, K.R., 1994. ISOPLOT — a plotting and regression program for radiogenic-isotope data. Version 2.75. Revision of U.S.G.S. Open-File Report 91-445.

Min, M., Peng, X., Wang, J., Osmond, J.K., 2005. Uranium-series disequilibria as a means to study recent migration of uranium in a sandstone-hosted uranium deposit, NW China. Applied Radiation and Isotopes, 63, 115–125.

Osmond, J.K., Dabous, A.A., 2004. Timing and intensity of groundwater movement during Egyptian Sahara pluvial periods by U-series analysis of secondary U in ores and carbonates. Quat Res, 61, 85–94

Osmond, J.K., Dabous, A.A., Dawood, Y.H., 1999. U-series age and origin of two secondary uranium deposits, central Eastern Desert, Egypt. Econ. Geol., 94, 273–280.

Osmond, J.K., Ivanovich, M., 1992. Uranium series mobilization and surface hydrology. In: Ivanovich, M., Harmon, R.S. (Eds.), Uranium-series Disequilibrium: Application to Earth, Marine, and Environmental Sciences, 2nd ed. Oxford Sciences Publications, Oxford, 259–289.

Pękala, M., Kramers, J.D., Waber, H.N., 2010. $^{234}U/^{238}U$ activity ratio disequilibrium technique for studying uranium mobility in the Opalinus Clay at Mont Terri, Switzerland. Applied Radiation and Isotopes, 68, 984–992.

Pöllänen, R., Ikäheimonen, T.K., Klemola, S., Vartti, V.-P., Vesterbacka, K., Ristonmaa, S., Honkamaa, T., Sipilä, P., Jokelainen, I., Kosunen, A., Zilliacus, R., Kettunen, M., Hokkanen, M., 2003. Characterization of Projectiles Composed of Depleted Uranium. *Journal of Environmental Radioactivity*, 64, 133-142.

Ramebäck, H., Vesterlund, A., Tovedal, A., Nygren, U., Wallberg, L., Holm, E., Ekberg, C., Skarnemark, G., 2010. The Jackknife as an Approach for Uncertainty Assessment in Gamma Spectrometric Measurements of Uranium Isotope Ratios. Nuclear Instruments and Methods in Physics Research B: Beam Interactions with Materials and Atoms, 268/16, 2535–2538.

Rowe, P.J., Maher, B.A., 2000. Cold' stage formation of calcrete nodules in the Chinese Loess Plateau: evidence from U-series dating and stable isotope analysis. Palaeogeography, Palaeoclimatology, Palaeoecology, 157, 109–125.

Schirrmeister, L., Oezen, D., Geyh, M.A., 2002. $^{230}Th/U$ Dating of Frozen Peat, Bol'shoy Lyakhovsky Island (Northern Siberia). Quaternary Research, 57, 253–258

Scholz, D., Hoffmann, D., 2008. $^{230}Th/U$-dating of fossil corals and speleothems. Eiszeitalter und Gegenwart, Quaternary Science Journal, 57/1–2, 52–76

Simpson, J., Grün, R., 1998. Non-Destructive Gamma Spectrometric U-Series Dating. Quaternary Geochronology, 17, 1009-1022.

Stoulos, S., Manolopoulou, M., Papastefanou, C., 2003. Assessment of natural radiation exposure and radon exhalation from building materials in Greece. J. Environ. Radioact., 69, 225-240.

Sutherland, R.A., de Jong, E., 1990. Statistical Analysis of Gamma-Emitting Radionuclide Concentrations for Three Fields in Southern Saskatchewan, Canada. Health Physics, 58/4 (April), 417-428.

Szabo, B.I., Haynes, C.V., Maxwell, T.A., 1995. Ages of Quaternary pluvial episodes determined by uranium-series and radiocarbon dating of lacustrine deposits of Eastern Sahara. Palaeogeography, Palaeoclimatology, Palaeoecology, 113, 227-242

Taçon, P.S.C., Aubert, M., Gang, L., Decong, Y., Hong, L., May, S.K., Fallon, S., Xueping, J., Curnoe, D., Herries, A.I.R., 2012. Uranium-series age estimates for rock art in southwest China. *Journal of Archaeological Science*, 39, 492-499

Thiel, K., Vorwerk, R., Saager, R., Stupp, H.D., 1983. ^{235}U fission tracks and ^{238}U-series disequilibria as a means to study recent mobilization of uranium in Archaean pyretic conglomerates. Earth Planet. Sci. Lett., 65, 249–262.

Wedepohl, H.K., 1995. The composition of the continental crust. – Geochimica et Cosmochimica Acta, 59, 1217-1232.

Wirsig, C., Kowsmann, R.O., Miller, D.J., Godoy, J.M.deO., Mangini, A., 2012. U/Th-dating and post-depositional alteration of a cold seep carbonate chimney from the Campos Basin offshore Brazil. Marine Geology, 329–331, 24–33.

Yokoyama, Y., Falguères, C., Sémah, F., Jacob, T., Grün, R., 2008. Gamma-Ray Spectrometric Dating of Late Homo Erectus Skulls from Ngandong and Sambungmacan, Central Java, Indonesia. *Journal of Human Evolution*, 55, 274–277.

Yücel, H., Solmaz, A.N., Köse, E., Bor, D., 2010. Methods for Spectral Interference Corrections for Direct Measurements of ^{234}U and ^{230}Th in Materials by Gamma-Ray Spectrometry. Radiation Protection Dosimetry, V. 138, No. 3, 264–277. doi:10.1093/rpd/ncp239.

Yücel, H., Cetiner, M.A., Demirel, H., 1998. Use of the 1001 keV Peak of ^{234m}Pa Daughter of ^{238}U in Measurement of Uranium Concentration by HPGe Gamma-Ray Spectrometry. Nuclear Instruments and Methods in Physics Research, Section A, 413, 74-82.

Zhao, J., Yu, K., Feng, Y., 2009. Review, High-precision ^{238}U–^{234}U–^{230}Th disequilibrium dating of the recent past: a review. Quaternary Geochronology, 4, 423–433.

TSSN 0976-3031